Polymer 50 (2009) 3095–3102

Contents lists available at ScienceDirect

Polymer

journal homepage: www.elsevier.com/locate/polymer

Synthesis of hybrid TiO_2 nanoparticles with well-defined poly(methyl methacrylate) and poly(tert-butyldimethylsilyl methacrylate) via the RAFT process

Van Giang Ngo [a], Christine Bressy [a,*], Christine Leroux [b], André Margaillan [a]

[a] Laboratoire MAtériaux-Polymères-Interfaces-Environnement Marin (EA 4323 MAPIEM), Avenue Georges Pompidou, BP 56, 83162 La Valette du Var, France
[b] IM2NP, UMR 6242 CNRS – Universités d'Aix-Marseille Paul Cézanne, Provence et Sud Toulon Var, BP 20132, 83957 La Garde Cedex, France

ARTICLE INFO

Article history:
Received 5 January 2009
Received in revised form
23 April 2009
Accepted 27 April 2009
Available online 15 May 2009

Keywords:
Hybrid nanocomposite
RAFT polymerization
"Grafting through" method

ABSTRACT

Surface of titania nanoparticles (TiO_2) was modified by a coupling agent as 3-(trimethoxysilyl)propyl methacrylate (MPS) to form TiO_2-MPS polymerizable particles. Methyl methacrylate (MMA) and tert-butyldimethylsilyl methacrylate (MASi) were radically polymerized through the immobilized vinyl bond on the surface in the presence of the reversible addition-fragmentation chain transfer (RAFT) agent 2-cyanoprop-2-yl dithiobenzoate using 2,2′-azobisisobutylnitrile (AIBN) as an initiator. FTIR spectroscopy confirmed the presence of the coupling molecule and the methacrylate groups on the surface. Thermogravimetric analysis and elemental analysis revealed a surface coverage of the coupling molecule of 2.0 wt%. TGA measurements showed that grafted PMMA and PMASi were accounted for 10% and 4.8% of the particle mass, respectively. ^{1}H NMR and SEC were used to verify the livingness of the polymerization. Transmission electron microscopy (TEM) was used to study the morphology of the particles before and after the surface grafting.

1. Introduction

The nanoscience and nanotechnology research works have veritably exploded over the last few years. Organic–inorganic or hybrid materials can be tailor-made with an infinite number of architectures and in diverse forms (monoliths, thin films, fibers, powders or particles). Core-shell polymers (organic/inorganic nanocomposites) have attracted increasing interest since they make it possible to control particle size and functionality. One of the best ways to avoid aggregation is to graft polymer chains onto the particles covalently, forming organic–inorganic hybrid materials. Those hybrid materials composed of inorganic core and organic polymer shell have intrigued interest for the combination of the properties of both the inorganic particles and the polymer such as solubility and easy processing [1].

A variety of polymerization methods, including conventional free radical [2,3], cationic [4–6], anionic [7–10], ring-opening [11,12], and controlled radical polymerizations (CRPs) have been used to graft the polymers onto the surface of different inorganic particles. Among those different methods, CRPs reveal advantages including the control of the macromolecular architecture, the molecular weight and its distribution in comparison with the conventional radical polymerization. They are simple on operation procedure and versatile on monomers in comparison with ionic polymerizations. Among the CRPs, nitroxide-mediated polymerization (NMP) [13–17] and atom transfer radical polymerization (ATRP) [18–20] have been used to graft polymers from solid surface and onto the solid surface. Comparing to the NMP and ATRP, the reversible addition-fragmentation chain transfer (RAFT) polymerization displays the advantage on compatibility with a wide range of monomers including functional monomers and with no contamination of free transition metal ion. Up to date, RAFT polymerization has been successfully used to graft various polymer chains onto different solid surfaces [21–36]. The overall RAFT polymerization is generally divided into two sets of reactions, that is, the so-called pre-equilibrium, which involves the initial RAFT agent and includes the initialization of the living process, and the main equilibrium between growing and dormant polymer chains [37].

Several methods of polymer grafting via the RAFT process are reported into the literature including the "grafting from" [21–30], "grafting to" [31–36], or "grafting through" methods [38]. Among them, the "grafting from" and "grafting through" methods allow monomer molecules to easily diffuse to the surface of the particles,

* Corresponding author. Tel.: +33 4 94 14 25 80; fax: +33 4 94 14 24 48.
E-mail address: christine.bressy@univ-tln.fr (C. Bressy).

0032-3861/$ – see front matter © 2009 Elsevier Ltd. All rights reserved.
doi:10.1016/j.polymer.2009.04.077

allowing higher graft density and better control of the molecular weight and polydispersity of the polymer chains [36,38]. Different ways of graft polymerization from the surface of particles including RAFT agent anchoring [21–30] or initiator anchoring [31] can be used via the RAFT process. Hojjati and Charpentier [27] grew polymer chains of methyl methacrylate from solid surfaces of titanium dioxide nanoparticles using 4-cyano-4-(dodecylsulfanylthiocarbonyl) sulfanyl pentanoic acid as RAFT agent to form TiO_2/PMMA nanocomposites. Hojjati et al. [30] grafted poly(acrylic acid) (PAA) on the surface of TiO_2 in using the same RAFT agent. In addition, various polymers such as poly(styrene) (PS) [21–23], poly(methyl methacrylate) [21–28], and poly(N-isopropylacrylamide) [28,29] have been successfully "grafted from" different surfaces via the RAFT process. In contrast with the "grafting from" method, the "grafting through" method uses a polymerizable coupling agent [23]. Few research works were reported in the literature to graft polymers on titanium dioxide nanoparticles and none of these papers used the RAFT polymerization. Chinthamanipeta et al. [38] grafted recently PMMA on the surface of silica using methacrylate-functionalized nanoparticles and RAFT polymerization. They claimed that by using the "grafting through" method, the same silica content can be used to get various desired molecular weight with the same amount of particles. This could be an advantage in contrast with the "grafting from" method where the RAFT agent and the particles content are linked.

This study involves the use of RAFT polymerization in the "grafting through" method. The 3-(trimethoxysilyl)propyl methacrylate (MPS) was used as a coupling molecule to anchor the polymer chains on the surface. Core-shell typed TiO_2-polymers were prepared. Methyl methacrylate (MMA) and a methacrylic monomer containing a hydrolytically labile bond such as the tert-butyldimethylsilyl methacrylate (MASi) were grafted on the nanoparticles surface. This is the first report of grafting such polymers to the surface of MPS-modified titanium dioxide nanoparticles by the "grafting through" method using the RAFT process.

2. Experimental section

2.1. Materials

The coupling agent, 3-(trimethoxysilyl)propyl methacrylate (MPS) (98% purity, 1.045 g/ml), and titanium(IV) dioxide nanopowder (TiO_2) (99.9% of purity, with a density of 3.8 g/cm^3 at 25 °C and a median particles size from 10 to 100 nm, together with an average diameter of particles of 55 nm assessed by X-ray diffraction and a subsequent specific surface area of 28.7 m^2/g) were received from Sigma–Aldrich. Reagent grade of ammonia (28 wt%) and ethanol was used as received. Toluene and methyl methacrylate (MMA) monomer were distilled under reduced pressure to remove the inhibitor before polymerization. 2,2′-Azobis(isobutyronitrile) (AIBN) was recrystallized with ethanol before used. The 2-cyanoprop-2-yl dithiobenzoate (CPDB) chain transfer agent (CTA) was synthesized according to the literature [39]. Tert-butyldimethylsilyl methacrylate (MASi) was synthesized as previously reported by Nguyen et al. [40].

2.2. Surface modification of nanoparticles with MPS

2.2.1. Method I

Silane grafting reaction onto the surface of oxide nanoparticles was carried out in ethanol as described by Rong et al. [41]. Titanium dioxide nanopowder (5 g) was dispersed in 108 ml of ethanol and 2.83 g of water, 1.52 g of ammonia (28 wt%) and 2.52 g of MPS were added. The mixture was stirred at room temperature for 1 h. 25 ml of solution was slowly distilled off under magnetic stirring at 105 °C, then residual of solvent was distilled at ambient temperature under reduced pressure. The dispersion was purified from free MPS and water or ammonia by centrifugation in absolute ethanol. The redispersion and centrifugation were repeated until no MPS could be detected by FTIR in the ethanol solution after centrifugation. The product was dried under vacuum at 30 °C for 24 h. The experiment has been performed three times noted TiO_2MPSI-1, TiO_2MPSI-2 and TiO_2MPSI-3, respectively.

Table 1
Experimental data obtained for the surface modification of nano-TiO_2 particles with MPS from Methods I and II.

Experiment	m_{MPS} (g)/m_{TiO_2} (g)
Method I	
TiO_2MPSI-1	2.52/5
TiO_2MPSI-2	2.52/5
TiO_2MPSI-3	2.52/5
TiO_2-5-MPS[a]	0.25/5
TiO_2-10-MPS[a]	0.5/5
TiO_2-20-MPS[a]	1.0/5
TiO_2-30-MPS[a]	1.5/5
TiO_2-40-MPS[a]	2.0/5
TiO_2-50-MPS[a]	2.50/5
TiO_2-100-MPS[a]	5/5
Method II	
TiO_2MPSII-1	2.5/5

[a] TiO_2-*X*-MPS where *X* represents the weight percentage of MPS added to 5 g of nano-TiO_2 particles.

2.2.2. Method II

Silane grafting reaction onto surface of TiO_2 nanoparticles was prepared in acetone, in using maleic anhydride as a catalyst [42]. In detail, titanium dioxide nanoparticle (10 g), and 3-(trimethoxysilyl)propyl methacrylate (MPS, 5 g) were dispersed in acetone (200 ml). The mixture was vigorously stirred at room temperature for 1 h then in boiling acetone (at 60 °C). 0.15 g of maleic anhydride, diluted in 1 ml water was added as a catalyst. The dispersion was refluxed for 2 h, and purified from free MPS by centrifugation. The redispersion and centrifugation were repeated until no MPS could be detected by FTIR in the acetone solution after centrifugation. The product was dried under vacuum at 30 °C for 24 h.

Both methods are listed in Table 1. The presence of the coupling agent MPS on the surface of oxide particles was confirmed by FTIR spectroscopy, and the amount of MPS grafted on the surface of oxides was determined by thermogravimetric analysis (TGA) and elemental analysis.

2.3. Grafting of MMA and MASi to the MPS-modified TiO_2 nanoparticles via the RAFT process

The reaction polymerization was conducted in toluene solution at 70 °C with a monomer concentration of 1.5 mol/l and a molar ratio of monomer/CTA/AIBN equals to 50:1:0.2. The theoretical number-average molecular weight is 10,000 g mol^{-1} (see Table 2).

Table 2
Experimental conditions for RAFT polymerizations of MMA and tert-butyldimethylsilyl methacrylate (MASi) with MPS-modified nano-TiO_2 particles.

	MMA	MASi
TiO_2MPSI-1 (g)	2	2
Monomer (mmol)	37.5	37.5
CPDB (mmol)	0.0375	0.075
AIBN (mmol)	0.0075	0.015
Precipitated solution	n-Pentane	Methanol

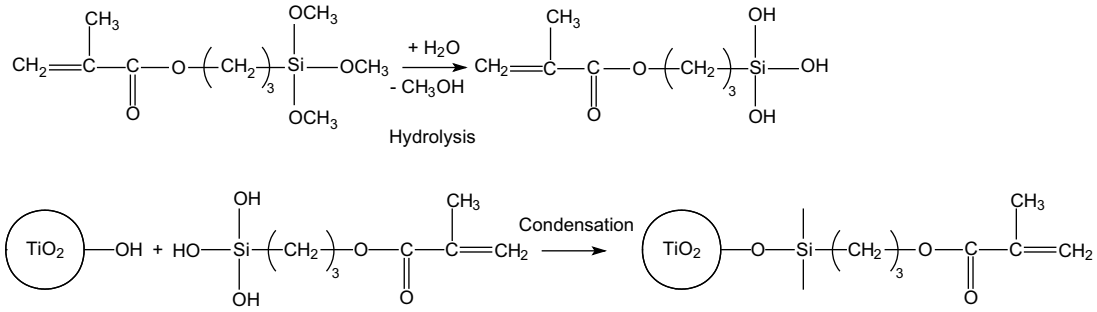

Scheme 1. Surface modification of TiO_2 nanoparticles by the coupling molecule 3-(trimethoxysilyl)propyl methacrylate (MPS).

Typically, in a 100 ml flask equipped with a magnetic stirrer, a toluene solution of monomer, titanium dioxide modified by MPS (TiO_2MPSI-1), CPDB, and AIBN was stirred for 1 h. The solution was degassed by three freeze-thaw-pump cycles by nitrogen liquid, filled with argon, and then placed in an oil bath previously heated at 70 °C. The solution was stirred and heated for 48 h. After 48 h, the reaction was stopped and cooled by nitrogen liquid. The reaction mixture was divided in two parts by centrifugation. The first part containing the grafted nanoparticles was washed several times with toluene to remove the free homopolymer chains, and dried in vacuo. Then, the toluene solution was poured into a non-solvent to precipitate the free homopolymer chains. After drying under vacuum, the product was characterized by SEC and ^{1}H NMR.

2.4. Characterization

The characterizations of MPS-modified and grafted particles were performed on a TGA–DSC instruments-Q600 from TA Instrument. The samples were heated under nitrogen (N_2) at a rate of 10 °C/min, from 30 °C to 800 °C and equilibrate at 30 °C for 5 min. Fourier Transform Infra-Red spectroscopic (FTIR) measurements were realized on a Thermo-Nicolet-Nexus spectrometer. The samples were prepared in KBr pellets with a weight content of 1%. The weight percentages of carbon and hydrogen atoms were assessed by elemental analysis performed at Vernaison, CNRS laboratory, France. The ^{1}H NMR spectra were recorded with a NMR Bruker advance 400-frequency: 400 MHz. $CDCl_3$ was used as deuterated solvent. The number-average molecular weight (M_n) and the molecular weight distribution or polydispersity index (PDI) of the polymer were determined at 30 °C on a SEC Waters 1515 HPLC pumps with THF as an eluent at a flow rate of 1.0 ml min^{-1}. The molecular weight and PDI data were assessed from a calibration with poly(methyl methacrylate) standards. Transmission electron microscopy images were taken using a Tecnai G2, operated at 200 kV ($\lambda = 2.51$ pm), with a point to point resolution of 0.25 nm. The powders were dispersed in ethanol, and a few drops put on a holey carbon grid. Images were taken from particles suspended over holes, in order to avoid any misinterpretation with the amorphous carbon film of the grid.

3. Results and discussion

3.1. Modification of nano-TiO_2 particles with MPS

Rong et al. [41] and Bauer et al. [42] have described experimental conditions used to anchor 3-(trimethoxysilyl)propyl methacrylate onto the surface of oxide particles. The reaction which occurs is depicted in Scheme 1. Methoxy groups of the MPS are hydrolyzed in the presence of base (Method I) or acid (Method II) to give silanol groups. The reactive trisilanol groups formed can be absorbed rapidly through condensation with the hydroxyl groups present on the TiO_2 surface to form Ti–O–Si bond linkages. This reaction results in the chemically bonded MPS to the nano-TiO_2 particle surface.

The covalent bond of MPS on the surface was determined through the use of FTIR spectroscopy. Blank samples containing 1% TiO_2 by weight in KBr were prepared, as well as samples containing the pristine MPS and the MPS-modified TiO_2 particles in KBr.

Fig. 1a–c shows the FTIR spectra in the 500–4000 cm^{-1} region. The absorption peaks of titanium dioxide are well separated from those of MPS. A strong absorption peak at 697 cm^{-1} attributed to

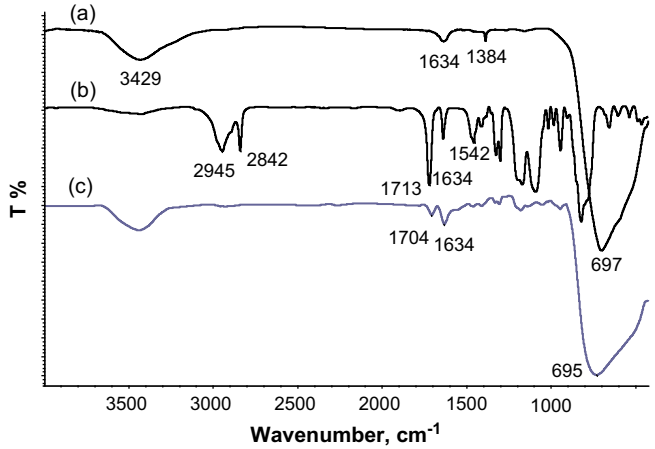

Fig. 1. FTIR spectra of (a) TiO_2 nanoparticles, (b) pure MPS, (c) MPS-modified TiO_2 from experiment TiO_2MPSI-2.

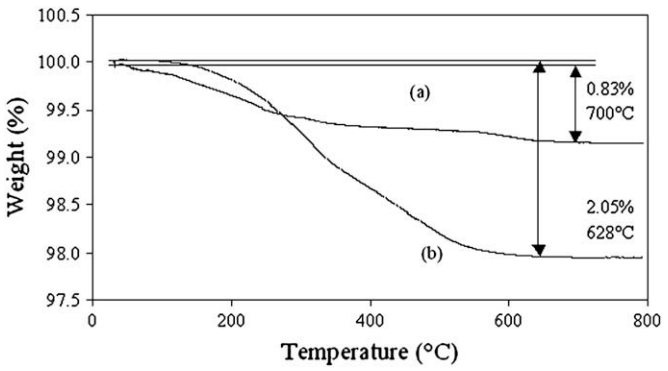

Fig. 2. TGA curves of (a) TiO_2 nanoparticles, (b) MPS-modified TiO_2 from experiment TiO_2MPSI-2.

Table 3
Values of the weight loss (%) (from TGA) and the weight percentage of MPS (from elemental analysis) onto TiO_2 nanoparticles.

Samples	Weight loss (%) from TGA	% wt (MPS)[a] from elemental analysis
TiO_2MPSI-1	2.05	1.70
TiO_2MPSI-2	2.29	1.85
TiO_2-100-MPS	4.04	4.33

[a] Calculated according to the equation $\%wt_{MPS} = (M_{MPS} \times \%wt(C)_{elemental\ analysis})/(N_C \times M_C)$, where, M_{MPS} is the molecular weight of MPS, %wt (C) the weight percentage of carbon, N_C the number of carbon atoms in MPS, and M_C the atomic mass of carbon.

Table 4
Values of the percentage of modification (p) and the grafting efficiency of MPS onto the surface of TiO_2 nanoparticles.

Samples	Weight loss of MPS (%) TGA	p (%)	Grafting efficiency (%)
TiO_2MPSI-1	2.05	1.23	2.47
TiO_2MPSI-2	2.29	1.47	2.96
TiO_2MPSI-3	2.08	1.26	2.53
TiO_2MPSII-1	2.27	1.45	2.94
TiO_2-5-MPS	1.62	0.80	16.13
TiO_2-10-MPS	1.79	0.97	9.80
TiO_2-20-MPS	1.81	0.99	2.00
TiO_2-30-MPS	1.92	1.10	3.71
TiO_2-40-MPS	1.72	0.90	2.27
TiO_2-50-MPS	1.90	1.08	2.18
TiO_2-100-MPS	4.04	3.22	3.33

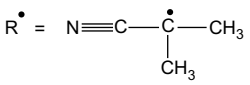

Scheme 2. Chemical structure of radicals generated from AIBN and CPDB.

Ti–O–Ti linkages in TiO_2 nanoparticles is observed. The broad absorption peaks at 3430 cm^{-1} and 1634 cm^{-1} are due to the stretching vibrations of the –OH groups on the surface of TiO_2 nanoparticles (Fig. 1a). The peak at 1384 cm^{-1} is due to the semi-crystalline anatase for $TiO_2 \cdot xH_2O$ [43,44]. For pure MPS (Fig. 1b), the peaks between 2481 and 2945 cm^{-1} are assigned to the stretching vibration of C–H bonds. The peak at 1713 cm^{-1} is assigned to the stretching vibration of the C=O. The peak at 1452 cm^{-1} is attributed to the methylene C–H bending vibration whereas the peak at 1407 cm^{-1} may be due to the vinyl C–H in plane bending vibration of MPS. The two well resolved peaks which appeared at around 1322 and 1300 cm^{-1} and the peak at 1170 cm^{-1} are assigned to –C–CO–O– skeletal vibration originating from the methacryloxy group [45]. For MPS-modified TiO_2 (Fig. 1c), the peak at 1704 cm^{-1} is assigned to the stretching vibration of the C=O groups of the MPS [46]. The peak of C=C at 1635 cm^{-1} could not be detected separately probably due to the overlapping with the strong peak of adsorbed water on the TiO_2 in the same frequency region. From these spectra, it can be deduced that the MPS coupling agent has been grafted on the surface of TiO_2 nanoparticles through the formation of covalent bonds. The methacrylate group of the MPS can further react with MMA and MASi via the RAFT process to form a polymer shell chemically bonded to the inorganic TiO_2 core.

To determine the weight amount of MPS on the nano-TiO_2 particles, TGA was performed on both the unmodified and surface treated TiO_2 particles (Fig. 2a and b). A weight loss of 0.83% for the unmodified TiO_2 may be assigned to the weight loss of the hydroxyl groups or adsorbed gases on TiO_2 nanoparticles. The weight loss of 2.05% for the MPS-modified TiO_2 (TiO_2MPSI-1) is close to the value of 1.7 wt% calculated from elemental analysis (Table 3). A similar observation is obtained for samples TiO_2MPSI-2 and TiO_2-100-MPS. Therefore, the percentage of modification (p) of nano-TiO_2 particles by MPS and the grafting efficiency were calculated from TGA using Eqs. (1) and (2).

$$p\,(\%) = (\text{Weight loss of MPS} - \text{TiO}_2) - (\text{Weight loss of TiO}_2) \quad (1)$$

$$\text{Grafting efficiency}\,(\%) = \frac{m_{\text{MPS grafted}}}{m_{\text{MPS introduced}}} \times 100 \quad (2)$$

where, $m_{MPS\ grafted} = p \times (m_{TiO_2}/(100 - p))$.

Results from Table 4 show the reproducibility of the modification of the nanoparticles by MPS through reactions of hydrolyzation and condensation with the hydroxyl groups under basic conditions (Method I). Similar weight amounts of MPS linked to the surface of TiO_2 are obtained for TiO_2MPSI-1, TiO_2MPSI-2, and TiO_2MPSI-3 samples. Moreover, the anchoring of MPS onto the surface of oxide particles under acidic conditions leads to similar weight amount around 2%. The percentage of modification (p) of nano-TiO_2 particles seems to increase with increasing the initial content of MPS for TiO_2-X-MPS samples. A maximum weight loss of 4.04% is obtained for TiO_2-100-MPS. The values of the grafting efficiency decrease with increasing the MPS/TiO_2 ratio in the mixture. Therefore, higher values of free MPS are obtained. This result demonstrates that the hydroxyl surface density (OH/nm^2) of the titania powders

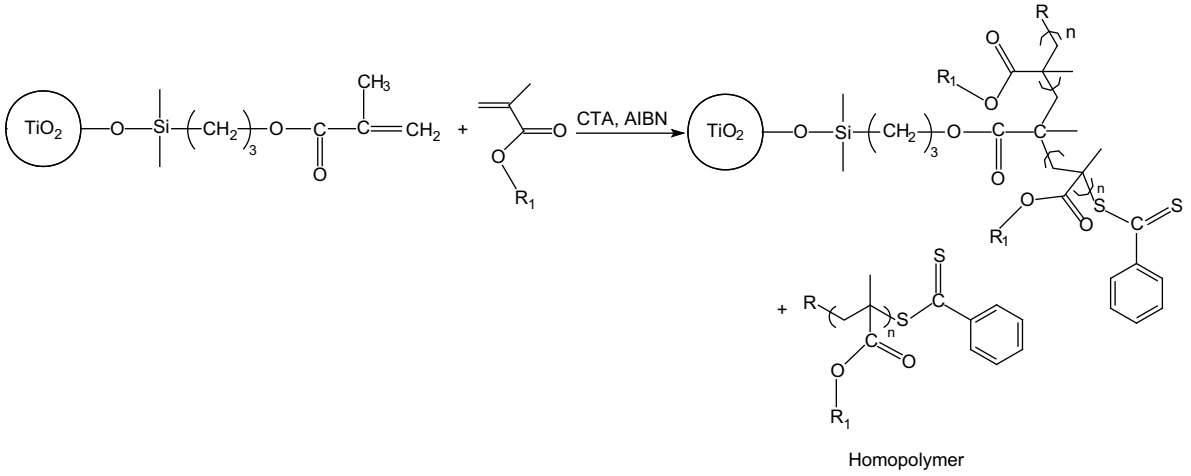

Scheme 3. Depiction of grafting methyl methacrylate and tert-butyldimethylsilyl methacrylate via the RAFT process through the surface of TiO_2 nanoparticles being functionalized with MPS. $R_1 = -CH_3$, for poly(methyl methacrylate) and $R_1 = -Si(CH_3)_2C(CH_3)_3$, for poly(tert-butyldimethylsilyl methacrylate).

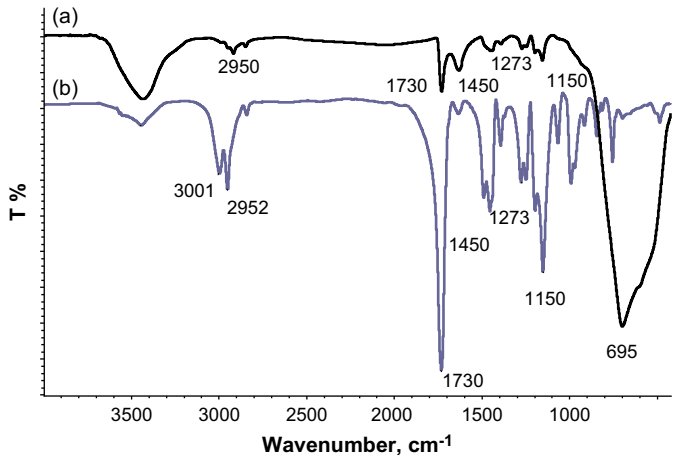

Fig. 3. FTIR spectra of (a) purified PMMA-TiO_2 nanoparticles and (b) pure PMMA.

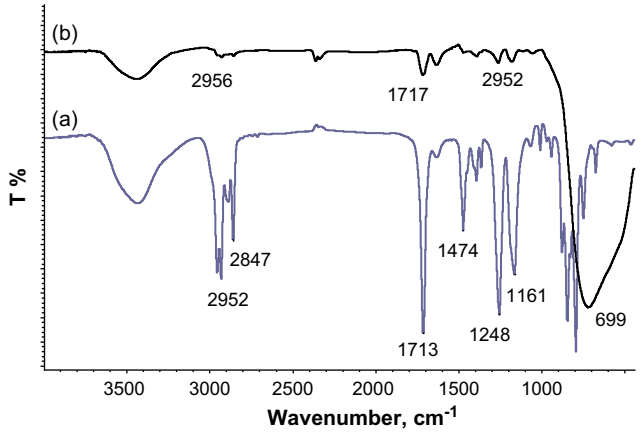

Fig. 4. FTIR spectra of (a) PMASi and (b) purified PMASi-TiO_2 nanoparticles.

is quite low limiting the value of the weight content of grafted MPS [47]. This value was estimated equal to 7 OH/nm^2 using the TGA weight loss from 120 °C to 500 °C and the specific surface area [48,49].

3.2. Grafting of MMA and MASi on MPS-modified nano-TiO_2 particles via the RAFT process

For the purposes of the "grafting through" method under RAFT conditions, a polymerizable double bond is immobilized on the surface of the nanoparticles. The RAFT agent or CTA is free in solution and could mediate the chain growth both in solution and at the particle surface. The vinyl group of the MPS can be cleaved via a radical way as well as the vinyl group of MMA or MASi in solution. Therefore, the functionalized-particle can react with the methyl methacrylate and tert-butyldimethylsilyl methacrylate monomers forming a polymer shell chemically bonded to the inorganic TiO_2 nanoparticle core. The mechanism involves the chain transfer of active species such as the radicals from decomposition of the initiator (AIBN) and propagating polymer radicals to the RAFT agent, forming an intermediate radical, followed by fast fragmentation to a polymeric RAFT agent and a new radical R$^{\bullet}$. This radical then continues polymerization. The equilibrium is established by subsequent chain transfer-fragmentation steps between the propagating radicals and polymeric RAFT agents and continues until all monomers are consumed, resulting in controlled growth of chains [37]. In our case, the radicals R$^{\bullet}$ from AIBN and CPDB have the same chemical structure as shown in Scheme 2. Unlike other grafting methods which produce a single chain extending normal to the surface, when chains are "grafted through", each anchor point could produce two arms extending from the surface as depicted in Scheme 3.

Fig. 3 shows the FTIR spectra of the nano-TiO_2 particles encapsulated by PMMA (a) and a pure PMMA (b). In the PMMA spectrum, the peak at 2952 cm^{-1} shows the C–H stretching and the peak at 1730 cm^{-1} is assigned to the carbonyl group of the ester function. The peak at 1440 cm^{-1} is due to the C–H bending and the peak at 1273 cm^{-1} can be assigned to the C–O stretching of the ester group [10]. The formation of PMMA-grafted TiO_2 nanoparticles is confirmed by the FITR spectrum shown in Fig. 3a, where the absorption peaks at 1150 cm^{-1} ($\nu_{-C-O-C-}$); 1730 cm^{-1} ($\nu_{-C=O}$) and 2952 cm^{-1} (ν_{-CH_3}) indicate the presence of PMMA macromolecules. In the same way of explanation, Fig. 4 shows the FTIR spectra of the pure PMASi and the nano-TiO_2 particles encapsulated by PMASi. In Fig. 4a, the peaks from 2856 to 2952 cm^{-1} and at 1713 cm^{-1} are assigned to the C–H (CH_2 and CH_3) stretching and the carbonyl group C=O, respectively. The peak located at 1474 cm^{-1} is due to C–H bending and the peak at 1248 cm^{-1} shows Si–C bonds coming from the ($Si(CH_3)_2$) group. The peak at 1161 cm^{-1} is assigned to –Si–O–C– bonds. The formation of PMASi-grafted-TiO_2 nanoparticles is confirmed by the FTIR spectrum through the presence of the following absorption peaks from 2847 to 2952 cm^{-1} (ν_{-C-H}) (CH_2 and CH_3), at 1717 cm^{-1} ($\nu_{-C=O}$), at 1260 cm^{-1} ($\delta_{-Si(CH_3)_2}$), and at 1179 ($\nu_{(-Si-O-C)}$).

While the presence of PMMA and PMASi on the surface was confirmed, the carbonyl peak is very small indicating that a small percentage of polymers had been grafted on the surface. Fig. 5 shows TGA curves of (a) pure PMMA and (b) purified PMMA-TiO_2

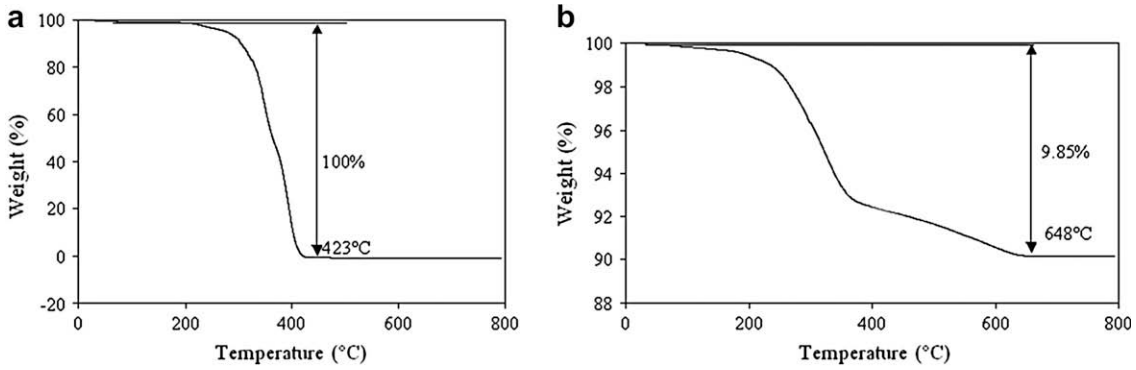

Fig. 5. TGA curves of (a) pure PMMA and (b) PMMA-grafted TiO_2.

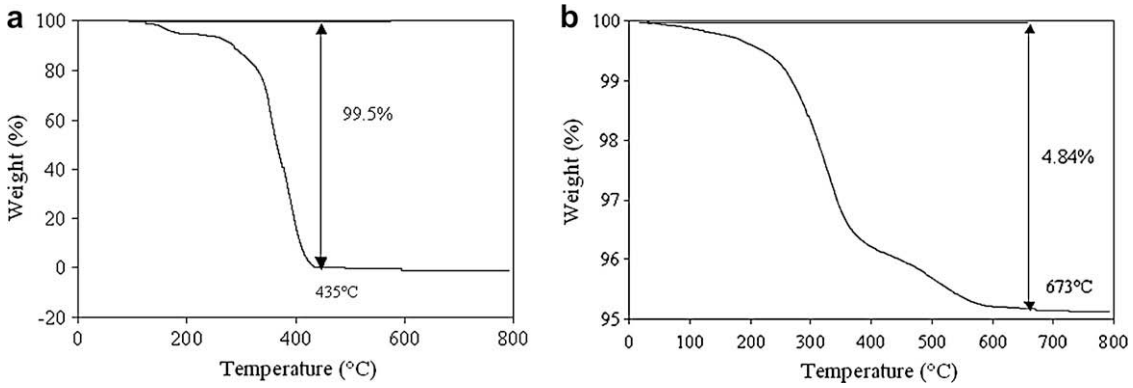

Fig. 6. TGA curves of (a) pure PMASi and (b) PMASi-grafted TiO_2.

Table 5
Results of MPS-modified TiO_2 nanoparticles (TiO_2MPSI-1) grafted by MMA and tert-butyldimethylsilyl methacrylate.

Polymer	Free homo-polymer (g)	Purified TiO_2-polymer nanoparticles (g)	Grafted polymer (g)	Grafting efficiency (%)
PMMA	2.27	2.22	0.22	9.69
PMASi	6.05	2.10	0.10	1.65

particles, under nitrogen atmosphere. It can be shown that the thermal degradation of PMMA occurs completely between 200 °C and 450 °C. For PMMA-grafted TiO_2 particles, a percentage of weight loss of 9.85% attributed to the grafted PMMA was found.

For PMASi-grafted TiO_2, the weight amount was around 4.8% (Fig. 6). From these values, the amount of grafted polymer chains can be estimated using Eq. (3).

$$\text{Grafted polymer (g)} = \frac{m_{\text{TiO}_2\text{–MPS introduced}} \times \%\text{weightloss(TGA)}}{1 - \%\text{weightloss (TGA)}} \tag{3}$$

Table 5 shows all the results obtained for the grafting of MPS-modified TiO_2 nanoparticles by MMA and tert-butyldimethylsilyl methacrylate via the RAFT process. Besides the grafting of polymer chains from the surface, homopolymer chains can be formed. We can see that the amount of free polymer chains is higher than the grafted polymer chains one. The "grafting through" method is found to be rather inefficient for PMASi in that only small amounts of polymer chains were able to be grafted to the surface (around 2 wt%). In both case, much less polymer chains were anchored onto the surface than were formed free in solution.

In addition, the grafting efficiency, defined in Eq. (4), is higher for the PMMA than for the PMASi. The hindered effect of the tri-alkylsilyl groups of the silylated monomer seems to decrease the ability of growing radicals to be linked to the surface in comparison with MMA.

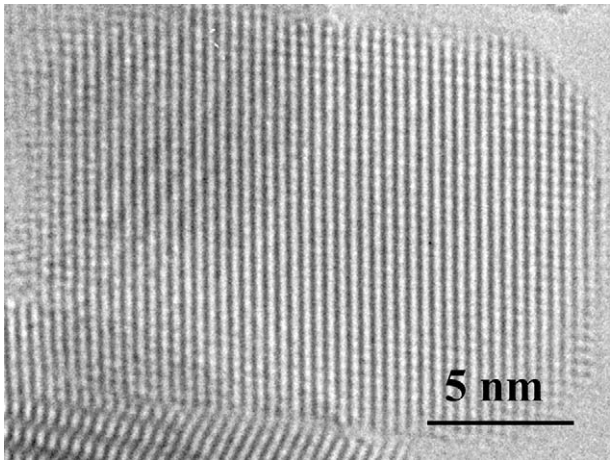

Fig. 7. Transmission electron micrographs of TiO_2 nanoparticles.

RAFT agent was anchored onto the surface of TiO_2 nanoparticles. Therefore, the concentration of the active RAFT agent on the TiO_2 surface is greater than in our situation where the RAFT agent is initially in solution.

The morphology of the ungrafted TiO_2 nanoparticles was studied by transmission electron microscopy and presented in Fig. 7.

Fig. 8a and b corresponds to the PMMA-grafted TiO_2 particles, as Fig. 8c and d corresponds to PMASi-grafted TiO_2. The TiO_2 particles have sizes varying from 10 to 100 nm, but whatever their sizes, and for the two types of polymers, one can found polymers surrounding the particles in comparison to Fig. 7. At low magnification (Fig. 8c), the particles embedded in polymers build bridges over the holes of the holey carbon grid. High Resolution Transmission Electron Microscopy (HRTEM) images (Fig. 8b and d) showed clearly the presence of the amorphous layer surrounding the particle. One can even see the amorphous contrast of the polymer superimposed to the lattice contrast of the crystallized particle (Fig. 8b). The thickness of the amorphous layer is irregular, varying 1.5–5 nm, whatever the polymer type.

$$\text{Grafting efficiency (wt\%)} = \frac{100 \times (\text{weight of polymer on inorganic particles})}{\text{Total weight of polymer formed}} \tag{4}$$

The grafting efficiency of PMMA through the surface of TiO_2 nanoparticles was 5 times less than the one proposed by Hojjati et al. [27] using the corresponding "grafting from" method. This difference can be explained by the fact that in this latter case, the

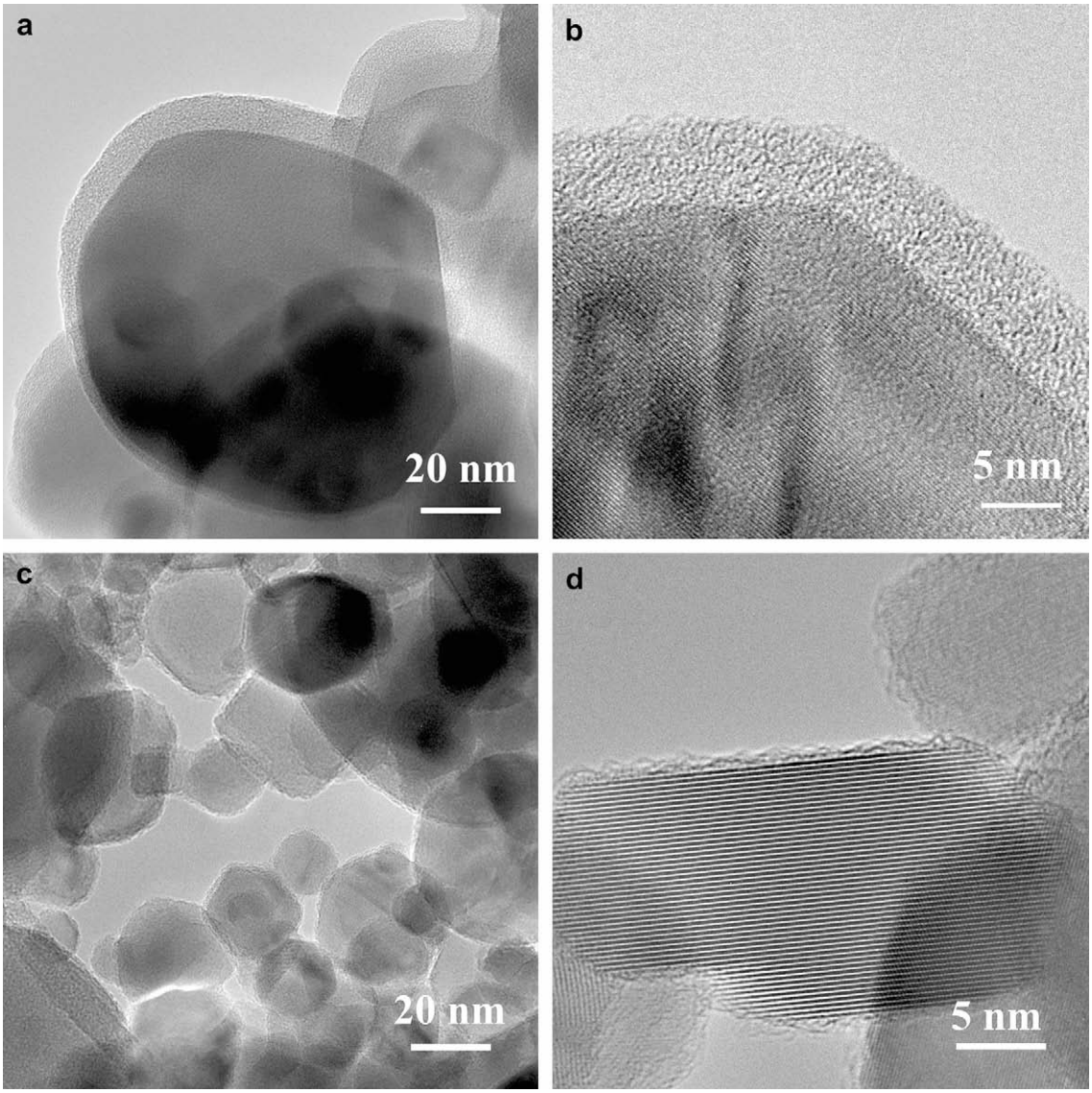

Fig. 8. Transmission electron micrographs of TiO_2 grafted particles. a) TiO_2 particles grafted with poly(methyl methacrylate). b) HRTEM image of (a), where the amorphous layer around the particle is visible, as well as on top of the particle. c) TiO_2 particles grafted with poly(tert-butyldimethylsilyl methacrylate) are stuck together by the polymer. d) HRTEM of one TiO_2 particle, showing the amorphous layer around the particle.

3.3. Control of the RAFT polymerization

The CPDB-mediated polymerizations of MMA and MASi onto the modified TiO_2 surface were done in toluene solution, at 70 °C. The molar ratio of the monomer to the CTA was calculated from Eq. (5), under the assumption that the efficiency of CPDB is 100% and termination events are negligible.

$$M_{n,th} = \frac{[\text{Monomer}]}{[\text{CTA}]} \times M_{\text{Monomer}} \times \text{Conv}_{\text{Monomer}} + M_{\text{CTA}} \qquad (5)$$

Table 6
Characteristics of the free PMMA and PMASi homopolymers derived from the RAFT polymerizations of MMA and MASi onto the MPS-modified TiO_2 nanoparticles.

Exp Nr.	Conv (%)	$M_{n,calc.}$ (g mol^{-1})	$M_{n,SEC}$ (g mol^{-1})	PDI
TiO_2MPSI-1-PMMA	76.2	7620	12,500	1.10
TiO_2MPSI-1-PMASi	89.9	8990	9500	1.12

where, $M_{n,th}$ is the theoretical number-average molecular weight (g mol^{-1}), M_{CTA} is the molecular weight of CTA and $\text{Conv}_{\text{Monomer}}$ is the monomer conversion.

For all polymerizations, $M_{n,th}$ was fixed at 10,000 g mol^{-1} for 100% of monomer conversion. As reported by Liu and Pan [50], the free homopolymer chains are expected to have the same M_n values as the corresponding anchored chains. Results from Table 6 show that the values of the number-average molecular weight of the free homopolymer chains were of the same magnitude as the calculated ones for both PMMA and PMASi homopolymers. In addition, low polydispersity indexes (<1.15) were obtained. This result demonstrates that the polymer chains have grown under control.

4. Conclusions

The synthesis of PMMA and PMASi grafted on the surface of TiO_2 nanoparticles via the RAFT process was found to be effective. The "grafting through" method was shown to be more efficient for grafting PMMA than PMASi polymer chains. Nevertheless, higher

amounts of free homopolymers were formed than anchored onto the surface of titania particles. TEM investigations on purified polymer-grafted TiO_2 nanoparticles demonstrated the presence of an amorphous layer corresponding to the polymer shell which covered the inorganic surface.

References

[1] Bourgeat-Lami E. In: Arshady R, Guyot A, editors. Dendrimers, assemblies and nanocomposites, vol. 5. London: Citus Book; 2002. p. 149–94 [chapter 5].
[2] Hajji P, David L, Gérard JF, Pascault JP, Vigier G. J Polym Sci Part B Polym Phys 1999;37:3172–87.
[3] Hsiue GH, Kuo WJ, Huang YH, Jeng RJ. Polymer 2000;41:2813–25.
[4] Jordan R, Ulman A. J Am Chem Soc 1998;120:243–7.
[5] Zhao B, Brittain WJ, Zhou W, Cheng S. J Am Chem Soc 2000;122:2407–8.
[6] Jang IB, Sung JH, Choi HJ, Chin I. Synth Met 2005;152:9–12.
[7] Mateva R, Ishtinakova O, Nikolov RN, Djambowa C. Eur Polym J 1998;34:1061–7.
[8] Jordan R, Ulman A, Kang JF, Rafailovich MH, Sokolov J. J Am Chem Soc 1999;121:1016–22.
[9] Zhou Q, Wang S, Fan X, Advincula R. Langmuir 2002;18:3324–31.
[10] Park BJ, Lee JY, Sung JH, Choi HJ. Curr Appl Phys 2006;6:632–5.
[11] Li W, Shen Z, Zhang Y. Eur Polym J 2001;37:1185–90.
[12] Chen J, Eberlein L, Langford CH. J Photochem Photobiol A Chem 2002;148:183–9.
[13] Zhao B. Polymer 2003;44:4079–83.
[14] Parvole J, Montfort JP, Billon L. Macromol Chem Phys 2004;205:1369–78.
[15] Bartholome C, Beyou E, Bourgeat-Lami E, Chaumont P, Lefebvre F, Zydowicz N. Macromolecules 2005;38:1099–106.
[16] Kobayashi M, Matsuno R, Otsuka H, Takahara A. Sci Tech Adv Mater 2006;7:617–28.
[17] Ghannam L, Parvole J, Laruelle G, Francois J, Billon L. Polym Int 2006;55:1199–207.
[18] Ejaz M, Yamamoto S, Ohno K, Tsujii Y, Fukuda T. Macromolecules 1998;31:5934–6.
[19] Matyjaszewski K, Miller PJ, Shukla N, Immaraporn B, Gelman A, Luokala BB, et al. Macromolecules 1999;32:8716–24.
[20] Carrnot G, Diamanti S, Manuszak M, Charleux B, Vairon JP. J Polym Sci Part A Polym Chem 2001;39:4294–301.
[21] Baum M, Brittain WJ. Macromolecules 2002;35:610–5.
[22] Skaff H, Emrick T. Angew Chem Int Ed 2004;43:5383–6.
[23] Salem N, Shipp DA. Polymer 2005;46:8573–81.
[24] Peng Q, Lai DMY, Kang ET, Neoh KG. Macromolecules 2006;39:5577–82.
[25] Wang LP, Wang YP, Wang RM, Zhang SC. React Func Polym 2008;68:643–8.
[26] Yuan K, Li ZF, Lu LL, Shi XN. Mater Lett 2007;61:2033–6.
[27] Hojjati B, Charpentier PA. J Polym Sci Part A Polym Chem 2008;46:3926–37.
[28] Raula J, Shan J, Nuopponen M, Niskanen A, Jiang H, Kauppinen EI, et al. Langmuir 2003;19:3499–504.
[29] Hong CY, You YZ, Pan CY. Chem Mater 2005;17:2247–54.
[30] Hojjati B, Sui R, Charpentier PA. Polymer 2007;48:5850–8.
[31] Baum M, Brittain WJ. Polymer Prepr 2001;42:586.
[32] Sumerlin BS, Lowe AB, Stroud PA, Zhang P, Urban MW, McCormick CL. Langmuir 2003;19:5559–62.
[33] Zorn M, Zentel R. Macromol Rapid Commun 2008;29:922–7.
[34] Daigle JC, Claverie JP. J Nanomater 2008:1–9.
[35] Jeon HJ, Go DH, Choi SY, Kim KM, Lee JY, Choo DJ, et al. Colloids Surf A Physicochem Eng Asp 2008;317:496–503.
[36] Aqil A, Vasseur S, Duguet E, Passirani C, Benoît JP, Roch A, et al. Eur Polym J 2008;44:3191–9.
[37] Moad G, Rizzardo E, Thang SH. Polymer 2008;49:1079–131.
[38] Chinthamanipeta PS, Kobukata S, Nakata H, Shipp DA. Polymer 2008;49:5636–42.
[39] Mitsukami Y, Donovan MS, Lowe AB, McCormick CL. Macromolecules 2001;34:2248–56.
[40] Nguyen MN, Bressy C, Margaillan A. J Polym Sci Part A Polym Chem 2005;43:5680–9.
[41] Rong Y, Chen HZ, Li HY, Wang M. Colloids Surf A: Physicochem Eng Asp 2005;253:193–7.
[42] Bauer F, Gläsel HJ, Decker U, Ernst H, Freyer A, Hartmann E, et al. Prog Org Coat 2003;47:147–53.
[43] Deng C, James PF, Wright PV. J Mater Chem 1998;8:153–9.
[44] Park HK, Kim DK, Hee C. J Am Ceram Soc 1997;80:743–9.
[45] Siddiquey IA, Ukaji E, Furusawa T, Sato M, Suzuki N. Mater Chem Phys 2007;105:162–8.
[46] Yang MY, Dan Y. Colloid Polym Sci 2005;284:243–50.
[47] Simmons GW, Beard BC. J Phys Chem 1987;91:1143–8.
[48] Mueller R, Kammler HK, Wegner K, Pratsinis SE. Langmuir 2003;19:160–5.
[49] Elshafei GMS, Philip CA, Moussa NA. Micropor Mesopor Mater 2005;79:253–60.
[50] Liu CH, Pan CY. Polymer 2007;48:3679–85.